Bioorganic & Medicinal Chemistry 19 (2011) 2991–2996

Contents lists available at ScienceDirect

Bioorganic & Medicinal Chemistry

journal homepage: www.elsevier.com/locate/bmc

Engineered *Thermoplasma acidophilum* factor F3 mimics human aminopeptidase N (APN) as a target for anticancer drug development

Jing Su [a], Qiang Wang [b,c], Jinhong Feng [b], Cong Zhang [a], Deyu Zhu [a], Tiandi Wei [a], Wenfang Xu [b,*], Lichuan Gu [a,*]

[a] *State Key Laboratory of Microbial Technology, Shandong University, Jinan 250100, China*
[b] *Department of Medicinal Chemistry, School of Pharmacy, Shandong University, Jinan 250012, China*
[c] *Department of Pharmaceutics, School of Life Sciences, South-Central University for Nationalities, Wuhan 430074, China*

ARTICLE INFO

Article history:
Received 16 January 2011
Revised 11 March 2011
Accepted 12 March 2011
Available online 21 March 2011

Keywords:
Aminopeptidase N
Inhibitors
Tricorn interacting factor F3
Crystal structure
Drug design

ABSTRACT

Human aminopeptidase N (hAPN) is an appealing objective for the development of anti-cancer agents. The absence of mammalian APN experimental structure negatively impinges upon the progression of structure-based drug design. Tricorn interacting factor F3 (factor F3) from *Thermoplasma acidophilum* shares 33% sequence identity with hAPN. Engineered factor F3 with two point directed mutations resulted in a protein with an active site identical to hAPN. In the present work, the engineered factor F3 has been co-crystallized with compound **D24**, a potent APN inhibitor introduced by our lab. Such a *holo*-form experimental structure helpfully insinuates a more bulky pocket than Bestatin-bound *Escherichia coli* APN. This evidence discloses that compound **D24** targetting the structure of *E. coli* APN cannot bind to the activity cleft of factor F3 with high affinity. Thus, there is a potential risk of inefficiency to design hAPN targeting drug while using *E. coli* APN as the target model. We do propose here now that engineered factor F3 can be employed as a reasonable alternative of hAPN for drug design and development.

1. Introduction

It needs to be spotlighted that cancer causes a fairly large number of deaths in the world every year. Metastasis is one of the intrinsic characteristics of malignant tumors, which often results in the clinical treatment failure and patient mortality.[1] Therefore, in the present climate, tumor metastasis in cancer therapy is becoming a challenging predicament, and how to efficiently restraint the invasion and metastasis of cancer cells is of indispensability for cancer medication.

Although there are many elements regarding the transfer process of the tumor cells' metastasis, the interaction between tumor cells and its surrounding micro-environment protein-degrading enzymes performs a critical portrayal. These enzymes comprise matrix metalloproteinases (MMPs), plasminogen and aminopeptidases (AP). Aminopeptidase N (APN) is related to the growth of primary tumor, second tumor and angiogenesis. It can also encourage tumor cell proliferation and differentiation.[2–5] All these interesting evidences make this enzyme an important target for drug design. The first known APN inhibitor, Bestatin (Ubenimex) extracted from *Streptomyces olivoreticuli*, was marketed in Japan in 1987 as an anti-neoplastic agent. In recent decades, some kinds of Bestatin analogues have been well developed, such as Probestin,[6] Amatatin,[7] Prebestatin,[8] etc. It is gold finger that the design of small molecules to target a specific protein can be greatly facilitated by experimental structure. However, the human aminopeptidase N (hAPN) crystal structure has not been determined so far. This troublesome condition frustrates the development of further specific drugs targeting hAPN. For that reason, homologous proteins with available 3D structure would contribute an applicable alternative.

Crystal structures of hAPN homologues, such as APN from *Escherichia coli* and its complex structure with Bestatin,[9,10] APN from *Neisseria meningitides*,[11] leukotriene A4 hydrolase (LTA4H) from human[12] and tricorn interacting factor F3 from *Thermoplasma acidophilum* (*T. acidophilum*),[13] have been determined recently. These crystallographic results provide appropriate awareness for APN research. At present time, the drug design targeting hAPN is generally depended on the three dimensional structures of these homologous proteins and enzyme-inhibitor models. However, structure-based sequence alignment analysis clearly exhibits that none of these proteins has identical active site with hAPN. Accordingly, drug design using these proteins' structures is undeniably not the best choice.

Tricorn interacting factor F3 (factor F3) from *T. acidophilum* has 33% sequence identity with hAPN. In particular, there are only two different residues between the active sites of factor F3 and of hAPN (Fig. 1). Point mutations of these two amino acids produce an

* Corresponding authors. Tel./fax: +86 531 88382264 (W.X.); tel./fax: +86 531 88362039 (L.G.).
E-mail addresses: xuwenf@sdu.edu.cn (W. Xu), lcgu@sdu.edu.cn (L. Gu).

0968-0896/$ - see front matter © 2011 Elsevier Ltd. All rights reserved.
doi:10.1016/j.bmc.2011.03.028

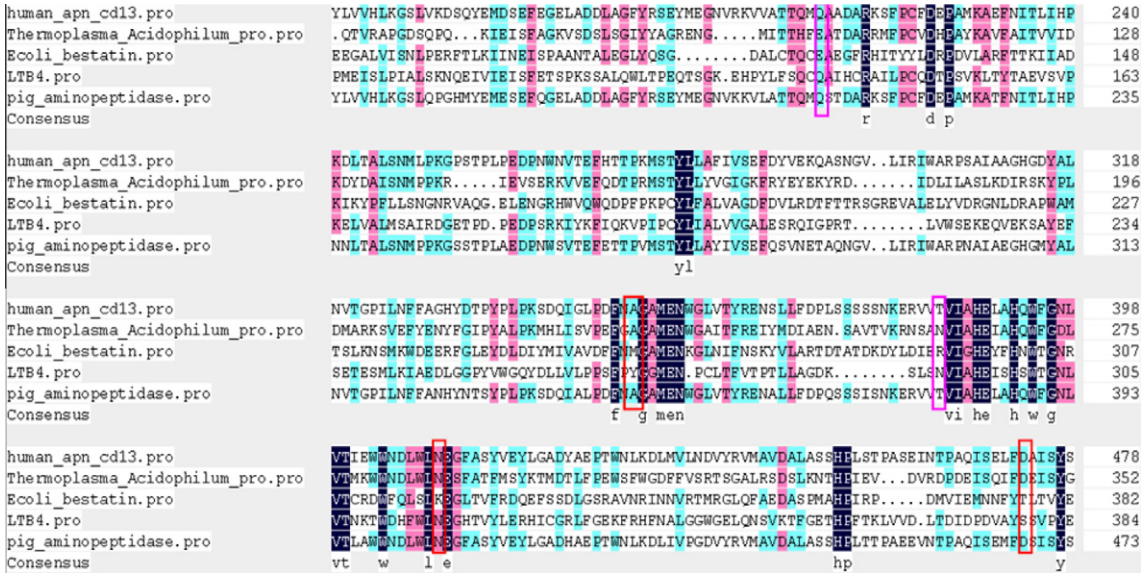

Figure 1. Sequence alignment of human aminopeptidase (hAPN) and homologous proteins. Structure-based sequence alignment of the hAPN, Susscrofa APN, *T. acidophilum* factor F3, human leukotriene A4 hydrolase and *E. coli* APN. The five important residues in the activity site are presented in pane. Residues conserved in hAPN and factor F3 are labeled in pink pane. Residues unconserved in hAPN and factor F3 are labeled in red pane.

active site for factor F3 identical to that of hAPN. Bestatin and other synthesized APN inhibitors also have inhibitory effect to the mutant factor F3 (Fig. S1). Thus, the 3D structure of such mutant protein could present a reasonable model for the downstream molecular design. Moreover, the *holo*-form crystal structure of this protein can be employed to determine the inhibitor-enzyme interaction as well as to design novel potent inhibitors.

Our group has long-term interest on the development of novel APN inhibitors. For example, we reported various series of APN inhibitors,[14–17] such as **B6**: *N*6-[(benzyloxy) carbonyl]-*N*2-(2,4-dichlorobenzoyl)-*N*1-hydroxy-L-lysinamide, a potent APN inhibitor equivalent to Bestatin,[14] and **D24**, which exhibits higher solubility than **B6**. In the current study we crystallized engineered factor F3 in complex with compound **D24** for deciding protein-inhibitor interaction and designing new efficient inhibitors. It should be noted that the crystal structure of such complex would demonstrate a plausible exemplary for anti-cancer drug design. Furthermore, the thermostablility of this engineered protein adjudicates that it can be the substitution for expensive and instable marketed APN during biological assay.

2. Experimental

E. coli strains were cultured at 37 °C in lysogeny broth (LB) and transformed as described previously.[18] *T. acidophilum* (ATCC25905™) was cultured in according to ATCC protocol. The plasmid pF3 native is the pET21b vector containing *T. acidophilum* factor F3. All biochemical reagents were purchased from Sigma (St. Louis, MO, USA).

2.1. Kinetics analytical method

The recombinant factor F3 mutant was purified by following the standard procedure as previously described.[10] Its APN activity was determined by measuring the absorbance increase at 405 nm of nitroanilide from the substrate (Leu-*p*-nitroanilide).[19] The reaction was incubated at 37 °C for 30 min. One unit of enzyme activity was defined as the amount of enzyme that causes an increase absorbance at 405 nm of 1 u/h.

Optimum temperature assay was performed as following procedures. Purified factor F3 mutant was mixed with the substrate Leu-*p*-nitroanilide then incubated for 30 min at 40, 50, 60, 65, 70, 80 and 90 °C, respectively. The activity was determined by measuring the absorbance increase at 405 nm.

Optimum pH of the enzyme was measured by using 50 mM acetic acid (pH 4–5.5), 50 mM MES (2-(*N*-morpholino) ethanesulfonic acid, pH 6–6.5) and 50 mM Tris–HCl (hydroxymethyl aminomethane hydrochloride, pH 7–9) then incubated at 37 °C for 30 min to measure the absorbance increase at 405 nm. The remaining session of the assay was done the same as the assay for enzyme optimum temperature.

2.2. Synthesis of D24

The synthetic scheme of target compound is depicted in Figure 2. Compound **5** was prepared as described by Wang et al.[14] After that, *N*-(*tert*-butoxycarbonyl)-L-phenylalanine (Boc-L-Phe) was conjugated to the –COOH of compound **5** by amidation to provide **6**. In the next step, the methyl ester **6** can be transformed to corresponding hydroximic acid **7** as per the methods mentioned before. Finally, the *N*-(*tert*-butoxycarbonyl)-protecting group of **7** can be cleaved with **3** *N* HCl in ethyl acetate to give hydrochloride salt of **D24**. White solid, yield 76.3%, mp 139–141 °C. MS (ESI) *m*/*z* $[M+H]^+$ 443.5; ^{1}H NMR (600 MHz, DMSO-d_6) δ 10.72 (s, 1H), δ 8.92 (s, 1H), δ 8.81 (d, J = 8.4 Hz, 1H), δ 8.11 (brs, 2H), δ 7.34 (m, 10H), δ 4.99 (s, 2H), δ 4.16 (dd, J_1 = 8.4 Hz, J_2 = 14.4 Hz, 1H), δ 3.79 (t, J = 7.2 Hz, 1H), δ 2.95 (m, 2H), δ 1.63 (m, 2H), δ 1.38 (m, 2H), δ 1.20 (m, 2H), δ 0.90 (m, 2H).

2.3. Enzyme inhibition comparison between factor F3 and APN

In the measurement of compounds inhibition constant on factor F3 mutants (E101Q, N261T), compounds were performed at the concentration 1280, 320, 80, 20, and 5 μg/mL in ddH_2O. The light absorbance changing with time was measured with a 96-well plate reader. To measure the inhibitory effect, the compounds and the enzyme were preincubated at 37 °C for 30 min prior to the addition of the substrate. The inhibition constant was analyzed with IC_{50}.

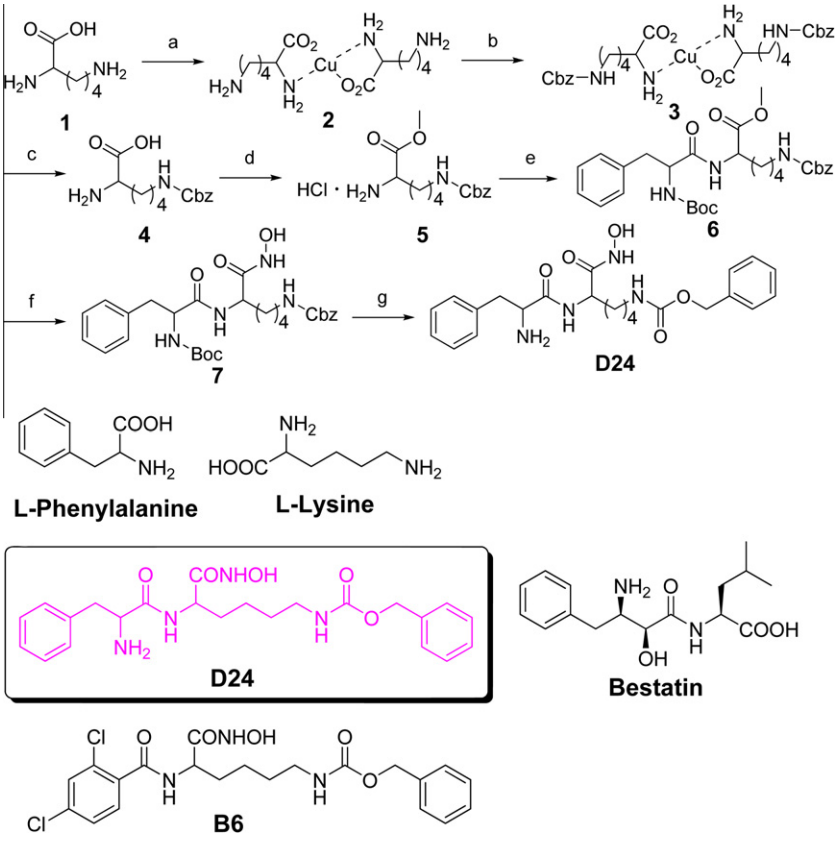

Figure 2. Reagents and reaction conditions: (a) $CuCO_3Cu(OH)_2$, 1.2 *N* HCl, H_2O, 80–90 °C, 2 h; (b) $NaHCO_3$, CbzCl, 25 °C, 12 h; (c) EDTA SS, 25 °C, 24 h; (d) MeOH, HCl, 25 °C, 6 h; (e) Boc-L-Phe, Et_3N, TBTU, CH_2Cl_2, 25 °C, 5 h; (f) NH_2OK, MeOH, 25 °C, 12 h; (g) HCl–EtOAc, 25 °C, 24 h.

2.4. Crystallization and data collection

Recombinant factor F3 mutant was concentrated to 10 mg/mL before crystallization. Crystals were grown by sitting-drop, vapor-diffusion method at 20 °C by mixing equal volume of protein complex with reservoir solution containing 0.1 M Tris-HCl (pH 8.5), 18% (w/w) PEG 2000, 0.2 M Li_2SO_4 and 1 mM compound **D24**. Diffraction data were collected at Shanghai Synchrotron Radiation facility (SSRF) beam line BL17u1. The data set were processed with HKL2000.[20] The X-ray data statistics are summarized in Table 1.

2.5. Structure determination and refinement

The crystal structure was solved by molecular replacement methods using the program Phaser in the CCP4 program suite[21] with *T. acidophilum* factor F3 (PDB entry: 1Z5H) as search model. The initial phase obtained from molecular replacement was further refined using PHENIX[22] and the model was rebuilt using COOT.[23] Data collection and structure refinement statistics are summarized in Table 1. All the molecular graphics figures were generated use PyMol (http://www.pymol.org). The structure has been deposited in the Protein Data Bank, access code: 3Q7J.

3. Results and discussion

3.1. Engineered F3 mutant (E101Q, N261T) has normal activity and is themostable

Structure-based sequence alignment discloses the factor F3 of *T. acidophilum* has only two amino acids different from the hAPN in

Table 1
X-ray data collection and refinement statistics

Parameters	F3-mutant with **D24**
Data collection	
Space group	*P*21212
a (Å)	114.7
b (Å)	183.1
c (Å)	105.2
α (°)	90
β (°)	90
γ (°)	90
Resolution (Å)	50–2.9
Total reflections	353272
Unique observations (outer shell)	49,142 (4287)
I/σ (outer shell)	16.13 (2.7)
R_{sym} (outer shell)[a]	0.128 (0.529)
Refinement	
Resolution range (Å)	50–2.9
Number of reflections ($\|F\|$ >0)	47,411
Data coverage (test set)	
$R_{working}/R_{free}$[b]	0.2024/0.2713
Total number of atoms	12,639
Root mean square deviation bond length (Å)	0.009
Bond angles (degree)	1.228
Ramachandran plot[c]	
Most-favored region (%)	90
Favored region (%)	8.5
Generously allowed region (%)	0.9
Disallowed region (%)	0.6

[a] $R_{sym} = \sum_{hkl}\sum_i|I(h\,k\,l)_i - \langle I(h\,k\,l)\rangle|/\sum_{hkl}\sum I\langle I(h\,k\,l)_i\rangle$ over *i* observations.
[b] Value of R_{free} for 1.91% of randomly selected reflections excluded from refinement.
[c] As defined in PROCHEK.[25]

active site. One is E101 substituted by Q in hAPN, and the other is N261 substituted by T. Site-directed mutations result in an engineered protein with active site identical to hAPN. To explore whether the engineered protein is druggable, biochemical characterization of this enzyme and compared the IC_{50}'s tendency between APN and engineered F3 mutant was well estimated. The experiments responded the K_m value of 62.453 μm (Fig. 3), which was higher than that of native factor F3 (34.7 μm).[24] The engineered protein divulges the maximum enzyme activity at 75 °C (Fig. 4) and pH 5.5 (Fig. 5) using Leu-NA as the substrate. The inhibitory tendency of four series of compounds (Bestatin, LYP,[26] A6,[27] **D24**) to engineered F3 mutant is accordance with APN. In another word, these molecules can suppress the F3 mutant's activity as well (Fig. S1). Consequently, our biochemical data evidently substantiated the feasibility of the substitution of hAPN by the engineered F3 protein.

3.2. Synthesis of D24 and evaluation of inhibitor

Our lab has unveiled numerous APN inhibitors, for example, **B6**: *N*6-[(benzyloxy) carbonyl]-*N*2-(2,4-dichlorobenzoyl)-*N*1-hydroxy-L-lysinamide that was equivalent to the positive control Bestatin.[14] Based on the compounds mentioned above, we designed the target compound **D24** that has better solubility than **B6**. The synthetic route of target compound is shown in Figure 2. The *N*6-amino group of L-lysine was selectively protected by Cbz (carbobenzoxy). Next, Boc-L-Phe was linked to the –COOH by amide bond to provide **6**. Then, the methyl ester **6** can be transformed to corresponding hydroximic acid **7** with methods mentioned before. Finally, the Boc-protecting group of **7** can be easily removed with 3 *N* HCl in ethyl acetate to give hydrochloride salt of **D24** (Fig. 2).

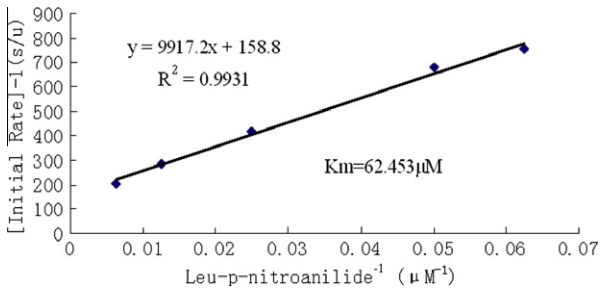

Figure 3. Enzyme assays of the factor F3 mutant with the substrate Leu-*p*-nitroanilide. Factor F3 mutant exhibits typical Michaelis–Menten enzymatic kinetics with a K_m constant of 62.45 μM for this substrate.

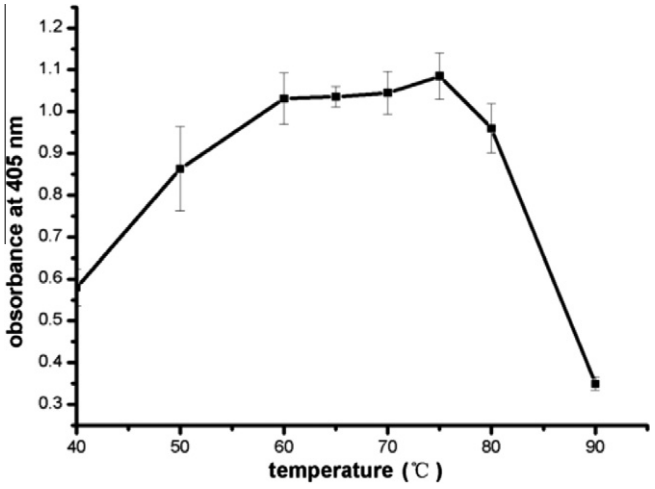

Figure 4. Effects of temperature on leucyl-*p*-nitroanilide hydrolysis by factor F3 mutant. The buffer used was 50 mM Tris–HCl (pH 8.0). The substrate and the enzyme were preincubated at 40, 50, 60, 65, 70, 75, 80 and 90 °C for 30 min and measured at 405 nm.

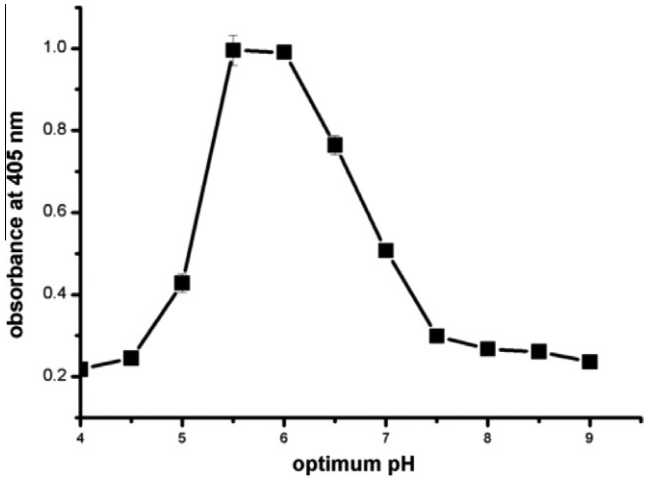

Figure 5. Effects of pH on leucyl-*p*-nitroanilide hydrolysis by factor F3 mutant. The buffers used were 50 mM acetic acid (pH 4–5.5), 50 mM MES (pH 6–6.5) and 100 mM tris-HCl (pH 7–9). The substrate and the enzyme were preincubated at 37 °C for 30 min to measure its absorbance at 405 nm.

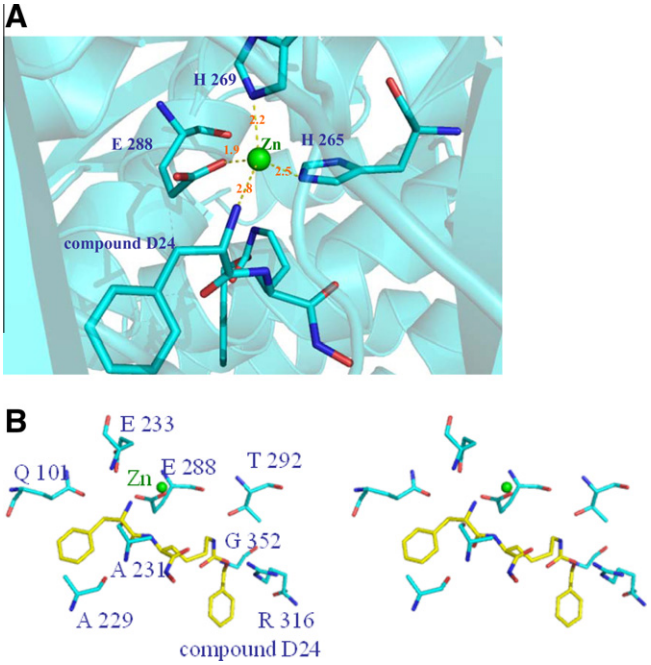

Figure 6. Stereo representation of the zinc-binding residues and interacted amino acids with compound **D24**. (A) The activity site of the factor F3 mutant with compound **D24**. Zinc ion was co-ordinated by H265, H269, E288 and compound **D24** molecule. These amino acids are labeled in cyan stick model and the distances are labeled with yellow dash. (B) Eight amino acids have interactions with the inhibitors. They are Q101, A229, A231, E233, E288, T292, R316 and G352. The compound **D24** is labeled with yellow stick, the zinc is labeled with green sphere and the eight amino acids are shown with cyan sticks.

Recombinant *T. acidophilum* factor F3 and the substrate of Leu-*p*-nitroanilide were used to evaluate the IC_{50} of the

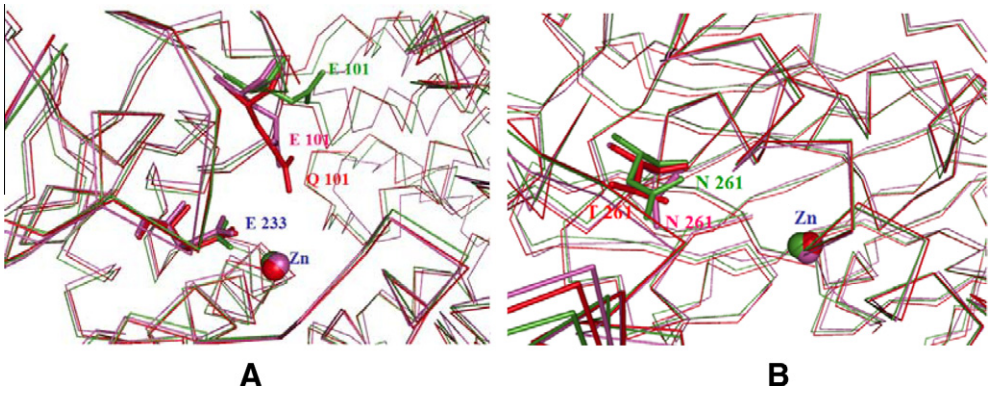

Figure 7. Structural comparison of factor F3 mutant with compound **D24** and F3 native crystal forms (PBD codes: 1Z1W and 1Z5H). Green ribbon represents the native crystal structure of 1Z1W; pink represents the native crystal structure of 1Z5H; red ribbon represents the factor F3 mutant (A, B). The amino acids are shown in different orientations with stick model and the zincs are shown in sphere model. (A) E101 mutant has an obvious conformational discrimination between the three structures. (B) N261 mutant increases the hydrophobicity of the surrounding environment.

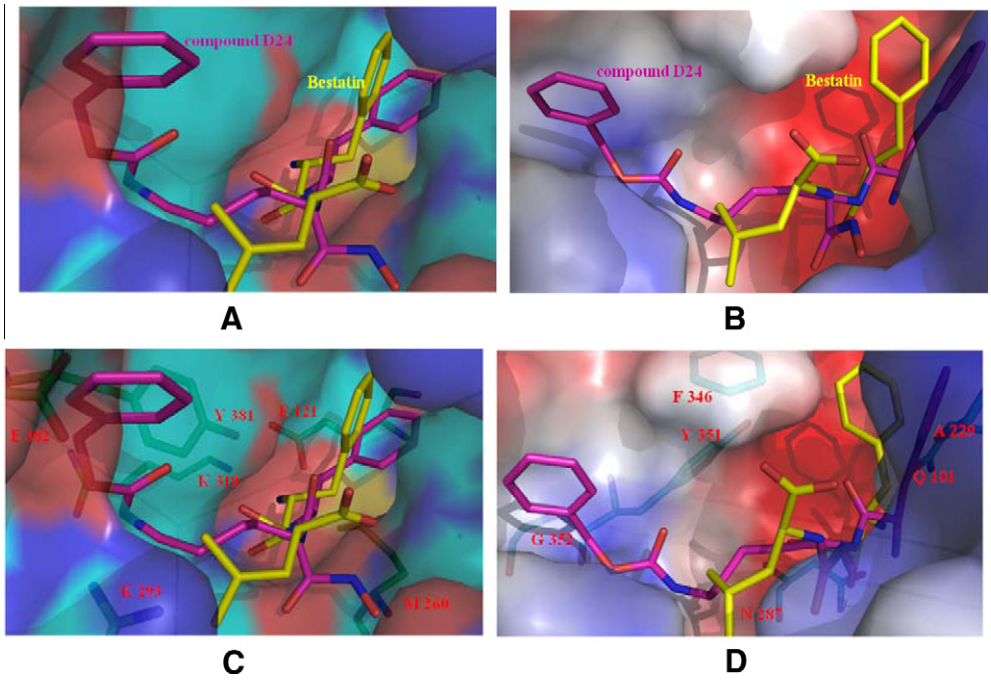

Figure 8. Binding pocket comparison of *E.coli* with Bestatin (PDB code: 2hpt) and factor F3 mutant with compound **D24**. (A) and (C) represent the *E. coli* structure. (B) and (D) represent the factor F3 mutant. Red represents negatively charged surfaces and blue represents positively charged surfaces, Bestatin is shown in yellow stick and compound **D24** is shown in purple stick model. (A) and (B) Electrostatic surface representation shows the clefts' shape between these two structures. *E. coli* with Bestatin has a narrower cleft than factor F3 mutant with compound **D24**. The cleft is narrower on the left where the N-terminus of the substrate binds and widens on the right to accommodate an extended polypeptide substrate. (C) and (D) The five amino acids at the binding pocket are different between the two structures. The amino acids (E382, R293, M260, K319 and E121) in *E. coli* at the binding pocket are different with hAPN. The amino acids (G352, N287, F346, A229 and 101N) aligned with *E. coli* are identical to hAPN.

synthesized compound **D24**. It showed the IC_{50} value of 30 μM for factor F3 mutants.

3.3. Analysis of the engineered factor F3 mutant protein-inhibitor interactions

3.3.1. The inhibitor occupies the active site of factor F3

The factor F3 is a zinc aminopeptidase. In the model of native protein, the catalytic zinc ion is coordinated by the N ε2 atoms of H265 and H269, a carboxylate oxygen atom of E288 and a water molecule.[10] The zinc-coordinating atoms form a close to a perfect tetrahedral coordination sphere with the zinc ion in the center. In our model, the zinc ion is coordinated by H265, H269, E288 and the amino group of compound **D24** (Fig. 6A). In the compound **D24** complex structure, there are eight amino acids interacting with the inhibitor: Q101, A229, A231, E233, E288, T292, R316 and G352 (Fig. 6B). The inhibitor is stabilized mainly by the combination of hydrophobic interaction and several hydrogen bonds.

Through superimposition of the two native structures (PDB codes: 1Z1W and 1Z5H) onto our compound **D24** complex structure, we found that the residue positions in active site exhibit dramatic change (Fig. 7A). In the two native structures, E101 adopts distinctive conformations. In 1Z1W, it adopts an outside orientation while in 1Z5H it is oriented to the inside but not quite extended due to the same charge repulsion with E233 that stand by. In our structure, the side chain of Q101 is buried inside deeply due to the loose of negative charge and stabilized by the inhibitor. The mutation of N261T does not cause conformational changes

except that it increases the hydrophobicity of its surrounding environment (Fig. 7B).

3.3.2. Engineered factor F3 mutant has a bigger substrate binding pocket than *E. coli* APN in complex with Bestatin

In the compound **D24** complex structure, a part of the inhibitor loses electron density. Thus the occupancy of compound **D24** in *T. acidophilum* factor F3 is not high. The compound **D24** is designed using *E.coli* aminopeptidase as a target model. This situation provokes a very essential issue on whether the structural differentation between *E. coli* APN and *T. acidophilum* factor F3 leads to a less-effective inhibitor. A structural comparison of the active sites of *E. coli* APN with Bestatin and factor F3 mutant with compound **D24** manifested that the former one (Fig. 8A) possesses narrower pocket to accommodate the inhibitor, whereas the later one is larger (Fig. 8B). This structural discrimination was mainly precipitated by the distinctive amino acids around the binding cavity (Fig. 8C, and D). At the substrate binding pocket, the replacement of G352 of *T. acidophilum* factor F3 concluded a bulky binding pocket. Furthermore, there are four additional different amino acids within these two proteins. Consequently, the inhibitor designed using *E. coli* APN as the model cannot tightly fasten the engineered *T. acidophilum* factor F3. Structure-based sequence alignment suggests that with these five amino acid substitutions, the engineered *T. acidophilum* factor F3 could be the best mimic of the hAPN as the drug design target.

4. Conclusions

An engineered factor F3 from *T. acidophilum* was planned to mimic hAPN as an anti-cancer drug target here now. A new protein generated by two point mutations on the native protein reveals an active site identical to the counterpart of hAPN. On the basis of this engineered protein, an known APN inhibitor, compound **D24**, exhibits inhibition activity. The protein-inhibitor interactions were characterized by biochemical and structural methods as well. According to our observation, the two residues (Q101 and T261) in point mutations experienced significant conformational changes in compound **D24** complex structure. This interesting evidence proposes that these two point mutations are necessary for the engineered protein to mimic hAPN. Subsequently, the comparison between *E. coli* APN with Bestatin and factor F3 mutant with compound **D24** demonstrated that the former has a slighter cleft than the factor F3 mutants. That's the reason that the inhibitor designed based on *E. coli* coordinate cannot securely buckle up the F3 mutant. Therefore, engineered factor F3 can be functioned as a satisfactory alternation of hAPN for drug design and screening. In conclusion, our structure would like to provide a brand new start point for the development of potent anti-cancer leads targeting hAPN.

Acknowledgements

We thank the staff at beam line BL17u1 at the Shanghai Synchrotron Radiation facility for support with data collection. This work was supported by State Key Laboratory of Microbial Technology, Shandong University and Grant of Hi-Tech Research and Development Program of China (2006AA02A324). We thank the support by National Nature Science Foundation of China (Grant No. 30772654 and No. 90713041) and National High Technology Research and Development Program of China (863 project; Grant No. 2007AA02Z314). We also thank support by special fund for Basic Scientific Research of Central Colleges, South-Central University for Nationalities (ZZQ10013).

Supplementary data

Supplementary data associated with this article can be found, in the online version, at doi:10.1016/j.bmc.2011.03.028.

Reference and notes

1. Liotta, LA.; Steeg, P. S.; Stetler-Stevenson, W. G. *Cell* **1991**, *64*, 327.
2. Dixon, J.; Kaklamanis, L.; Turley, H.; Hickson, I. D.; Leek, R. D.; Harris, A. L.; Gatter, K. C. *J. Clin. Pathol.* **1994**, *47*, 43.
3. Sato, Y. *Biol. Pharm. Bull.* **2004**, *27*, 1763.
4. Fujii, H.; Nakajima, M.; Saiki, I.; Yoneda, J.; Azuma, I.; Tsuruo, T. *Clin. Exp. Metastasis* **1995**, *13*, 337.
5. Saiki, I.; Fujii, H.; Yoneda, J.; Abe, F.; Nakajima, M.; Tsuruo, T.; Azuma, I. *Int. J. Cancer* **1993**, *54*, 137.
6. Aoyagi, T.; Yoshida, S.; Nakamura, Y.; Shigihara, Y.; Hamada, M.; Takeuchi, T. *J. Antibiot. (Tokyo)* **1990**, *43*, 417.
7. Rich, D. H.; Moon, B. J.; Harbeson, S. *J. Med. Chem.* **1984**, *27*, 417.
8. Yoshida, S.; Nakamura, Y.; Naganawa, H.; Aoyagi, T.; Takeuchi, T. *J. Antibiot. (Tokyo)* **1990**, *43*, 149.
9. Addlagatta, A.; Gay, L.; Matthews, B. W. *Proc. Natl. Acad. Sci. U.S.A.* **2006**, *103*, 13339.
10. Ito, K.; Nakajima, Y.; Onohara, Y.; Takeo, M.; Nakashima, K.; Matsubara, F.; Ito, T.; Yoshimoto, T. *J. Biol. Chem.* **2006**, *281*, 33664.
11. Nocek, B.; Mulligan, R.; Bargassa, M.; Collart, F.; Joachimiak, A. *Proteins* **2008**, *70*, 273.
12. Thunnissen Marjolein, M. G. M.; Par, Nordlund; Haeggstrom Jesper, Z. *Nat. Struct. Biol.* **2001**, *8*, 131.
13. Kyrieleis, O. J.; Goettig, P.; Kiefersauer, R.; Huber, R.; Brandstetter, H. *J. Mol. Biol.* **2005**, *349*, 787.
14. Wang, Q.; Chen, M.; Zhu, H.; Zhang, J.; Fang, H.; Wang, B.; Xu, W. *Bioorg. Med. Chem.* **2008**, *16*, 5473.
15. Zhang, Xiaopan; Fang, Hao; Zhu, Huawei; Wang, Xuejian; Zhang, Lei; Li, Minyong; Li, Qianbin; Yuan, Yumei; Wenfang, Xu *Bioorg. Med. Chem.* **2010**, *18*, 5775.
16. Li, Qianbin; Fang, Hao; Wang, Xuejian; Xu, Wenfang *Eur. J. Med. Chem.* **2010**, *45*, 1618.
17. Li, Qianbin; Fang, Hao; Wang, Xuejian; Hu, Liping; Wenfang, Xu. *Eur. J. Med. Chem.* **2009**, *44*, 4819.
18. Sambrook, J.; Fritsch, E. F.; Maniatis, T. *Molecular Cloning: A Laboratory Manual*, 2nd ed.; Cold Spring Harbor Laboratory Press: New York, 1989.
19. Herrera-Camacho, I.; Rosas-Murrieta, N. H.; Rojo-Dominguez, A.; Millan, L.; Reyes-Leyva, J.; Santos-Lopez, G.; Suarez-Rendueles, P. *FEBS J.* **2007**, *274*, 6228.
20. Otwinowski, Z.; Minor, W. *Methods Enzymol.* **1997**, *276*, 307.
21. Project, C. C. *Acta Crystallogr., Sect D* **1994**, *50*, 216.
22. Adams, P. D.; Grosse-Kunstleve, R. W.; Hung, L. W.; Ioerger, T. R.; McCoy, A. J.; Moriarty, N. W.; Read, R. J.; Sacchettini, J. C.; Sauter, N. K.; Terwilliger, T. C. *Acta Crystallogr., Sect. D Biol. Crystallogr.* **2002**, *58*, 1948.
23. Emsley, P.; Cowtan, K. *Acta Crystallogr., Sect. D Biol. Crystallogr.* **2004**, *60*, 2126.
24. Tamura, N.; Lottspeich, F.; Baumeister, W.; Tamura, T. *Cell* **1998**, *95*, 637.
25. Laskowski, Roman A.; MacArthur, Malcolm W.; Moss, David S.; Thornton, Janet M. *J. Appl. Crystallogr.* **1993**, *26*, 283.
26. Luan, Yepeng; Wang, Xuejian; Zhu, Huawei; Qu, Xianjun; Fang, Hao; Xu, Wenfang *Lett. Drug Des. Disc.* **2009**, *6*, 420.
27. Shang, L.; Fang, H.; Zhu, H.; Wang, X.; Wang, Q.; Mu, J.; Wang, B.; Kishioka, S.; Xu, W. *Bioorg. Med. Chem.* **2009**, *17*, 2775.